Commun. Optim. Theory 2027 (2027) 18 https://doi.org/10.23952/cot.2027.18

MATHRES Communications in Optimization Theory
Available online at http://cot.mathres.org

CONSTRUCTION OF MINIMAL SURFACES LYING OVER SHEARS OF SOME CONVEX DOMAINS

MADHUSMITA MOHANTY, BIKASH KUMAR CHINHARA*

Faculty of Science, Sri Sri University, Cuttack, Odisha, India

Dedicated to Professor Ram Mohapatra

Abstract. The Weierstrass–Enneper representation establishes a fundamental connection between harmonic mappings and isothermal parametrizations of minimal surfaces. In this article, we employ the harmonic shear technique to construct harmonic mappings that arise as projections of minimal surfaces. Specifically, we obtain novel minimal surfaces defined over the shears of convex domains, including the right half-branch of a hyperbola, the right half of the Lemniscate of Bernoulli, and the interior of a parabolic region. Furthermore, we investigate the corresponding conjugate and associated minimal surfaces derived from these constructions. Graphical illustrations are provided to support and visualize the theoretical results. These findings contribute to the growing interplay between geometric function theory and minimal surface theory.

Keywords. Harmonic mapping; Lemniscate of Bernoulli; Isothermal parameters; Minimal surface; Weierstrass-Enneper representation.

2020 Mathematics Subject Classification. 30C45, 30C50, 30C55.

1. INTRODUCTION

A surface that minimizes the area subject to a fixed boundary curve in $\mathbb{R}^3$ is termed a minimal surface. For any given curve in $\mathbb{R}^3$, infinitely many surfaces can be constructed having this curve as their boundary. Among all such surfaces, the one with the smallest surface area is termed a minimal surface. The existence of such a minimal surface was first conjectured by Joseph-Louis Lagrange in 1760, a problem now famously known as Plateau's problem. The problem was independently solved by Jesse Douglas and Tibor Radó in 1930. In the direction of explicit representation of a minimal surface, it has been less studied. Our primary focus in this article is to develop a class of mathematical expressions that yield minimal surfaces, which may aid in the design of models for various physical phenomena.

*Corresponding author.

E-mail address: mohantymadhu93@gmail.com (M. Mohanty), bikash.c@srisriuniversity.edu.in (B.K. Chinhara).

Received October 20, 2025; Accepted April 18, 2026.

©2027 Communications in Optimization Theory

A fundamental relationship exists between curvature and minimal surfaces: the mean curvature vanishes everywhere on a minimal surface. Minimal surfaces are a key component of the generative design toolbox used by modern designers. In architecture, there has been much interest in tensile structures, which are closely related to minimal surfaces. The most significant application of minimal surface theory in general relativity appears in the Schoen-Yau proof of the positive mass theorem. This theory is closely tied to chemical phenomena. Surfaces of zero potential formed in various salt solutions exhibit close approximations to periodic minimal surfaces, characterized by vanishing mean curvature, defined as the arithmetic mean of principal curvatures. Research has demonstrated that within biological systems, the predominant structural forms are minimal surfaces or close approximations thereof. Consequently, minimal surface theory finds extensive application in protein folding and DNA functionality studies. Furthermore, minimal surfaces elucidate numerous phenomena in natural science, architecture, and molecular engineering (see [1]).

Minimal surfaces minimize area locally. However, not every minimal surface necessarily minimizes global area. It is essential to note that minimal surfaces over convex domains are globally area-minimizing. This property does not necessarily hold for minimal surfaces over non-convex domains (see [8, 10, 13]). Sufficient conditions under which minimal surfaces in non-convex domains achieve global area minimization can be found in the work by Michael Dorff et al. [4]. When a minimal surface does not exhibit self-intersection, it may be interpreted as a minimal graph. Interestingly, this minimal surface or graph represents many natural phenomena and facilitates modeling various energy-minimizing physical processes. For modeling and extrapolating natural phenomena, the existence of classes of pre-established minimal surfaces is vital. Addressing these issues, the connection between harmonic functions and minimal surfaces is formalized through the renowned Weierstrass-Enneper representation theorem, which establishes the relationship between minimal surfaces defined by isothermal parameters and univalent harmonic functions (see [7, 14]). According to this fundamental result, the coordinate functions of a minimal surface in $\mathbb{R}^3$ represented in the isothermal parameters are harmonic. The literature contains studies of novel minimal surface constructions over various geometrical domains, including minimal surfaces over the upper half-plane, slanted half-planes, single slits, vertical strips, and regular n-gons. Therefore, our investigation focuses on constructing minimal surfaces over additional domains, specifically the interior of the right half-branch of a hyperbola, the right half-branch of the Lemniscate of Bernoulli, and domains bounded by parabolas, while identifying the corresponding minimal surfaces over these respective domains (see [6, 9, 12, 15]). Due to computational complexity, very little work has been done on unbounded convex domains. Our work primarily focuses on generating various classes of minimal surfaces, their conjugates, and associated minimal surfaces related to convex domains with unbounded boundaries. Recent work has strengthened the link between harmonic mappings and minimal surface theory. Bhowmik and Majee [2] provided curvature estimates for minimal surfaces generated by harmonic mappings with a nonzero pole, offering clearer geometric insight and motivating further study of surfaces produced by harmonic shears.

The following preliminaries concerning the theory of harmonic univalent mappings are required. We study a harmonic mapping as a function $f(z,\bar{z}) = u(x,y) + iv(x,y)$, $z = x+iy$, where both u and v satisfy the Laplace equation $\triangle u = 0$ and $\triangle v = 0$, where $\triangle$ is defined by $\triangle = \frac{\partial^2}{\partial x^2} + \frac{\partial^2}{\partial y^2}$, or equivalently satisfies $\nabla f = 0$, where $\nabla = 4\frac{\partial^2}{\partial z \partial \bar{z}}$. This function f can always

be represented with the help of two analytic functions h and g, $f = h + \overline{g}$, in a simply connected domain Ω. f is locally univalent if and only if the Jacobian of f, $J_f := |h'|^2 - |g'|^2$, is nonvanishing (due to Lewy [11]). A locally univalent harmonic mapping is sense-preserving or sense-reversing depending on whether $J_f > 0$ or $J_f < 0$, respectively, in the domain Ω. Since $h' \neq 0$, the analytic component h is locally univalent in the open unit disk $\mathbb{D} := \{z \in \mathbb{C} : |z| < 1\}$. The second complex dilatation $w := g'/h'$ of f constitutes an analytic function in $\mathbb{D}$ with $|w| < 1$.

The proofs of the main results employ the computational methodology commonly known as the shearing technique to construct new univalent harmonic mappings from existing univalent analytic functions (due to Clunie and Sheil-Small [3] Theorem 5.3). The philosophy of that result says, for a given (locally)univalent harmonic mapping, $f = h + \overline{g}$, we can conclude that global univalence of f in $\mathbb{D}$ onto a domain convex in horizontal direction (say Γ) is the consequence of the univalence of the analytic function $\phi := (h - g)$, in $\mathbb{D}$ onto Γ, and vice versa.

Another significant result from the studies of differential geometry is the well-known Weierstrass-Enneper representation theorem, which plays a crucial role in our results and is highlighted in the following theorem.

Theorem 1.1. *(Weierstrass Representation*[14]*) Let $\Omega \subset \mathbb{C}$ be a simply connected domain with $0 \in \Omega$, and let $f : \mathbb{D} \to \Omega$ be a harmonic univalent mapping of the form $f = h + \overline{g}$. Define the complex dilatation of f by*

$$w(z) = \frac{g'(z)}{h'(z)} = q^2(z),$$

where $q : \mathbb{D} \to \mathbb{C}$ is an analytic function. Then, the parametrization

$$X(z) = \left(Re\{h(z) + g(z)\}, Im\{h(z) - g(z)\}, 2Im\left\{ \int_0^z q(\zeta) h'(\zeta)\, d\zeta \right\} \right)$$

defines a minimal surface in $\mathbb{R}^3$ whose orthogonal projection onto the xy-plane is precisely $f(\mathbb{D})$. Moreover, up to rigid motions, this parametrization gives a unique minimal surface with the prescribed projection. Conversely, let S be a minimal surface given by a parameterization $\{(u, v, F(u, v)) : u + iv \in \Omega\}$ for some domain Ω. Then the projection mapping $f(z) = u + iv$ from $\mathbb{D}$ to Ω is harmonic and univalent, with dilatation $w(z) = q^2(z)$.

Furthermore, we introduce the terminology conjugate minimal surfaces of a minimal surface $X(u, v)$ as another minimal surface, namely $Y(u, v)$, such that the component functions of X and Y are pairwise harmonic conjugates. Next, we generate the one-parameter family of minimal surfaces from the two conjugate minimal surfaces X and Y by $Z(u, v) = (\cos t)X + (\sin t)Y$, $t \in \mathbb{R}$. For a fixed $t \in [0, \pi/2]$, we say the family of suface Z is the associated minimal surface of the minimal surfaces X and Y.

The following result due to Dorff and Muir [5] gives a computational tool to explicitly represent conjugate and associated minimal surface of a given minimal graph.

Theorem 1.2. *Let ϕ be a convex analytic function in $\mathbb{D}$ with $\phi(0) = 0$ and $\phi'(0) = 1$, and q be an analytic univalent function in $\mathbb{D}$ with $q(0) = 0$. Suppose that the univalent harmonic mapping $f : \mathbb{D} \to \mathbb{C}$ is defined by $f = h + \bar{g}$, and $\phi := h - g$, $\omega := g'/h' = q^2$, where $h(0) = g(0) = g'(0) = 0$ and $h'(0) = 1$. Then $f_t : \mathbb{D} \to \mathbb{C}$, $f_t := e^{it}h + \overline{e^{it}g}$, $t \in \mathbb{R}$ lift to a minimal graph*

$$X_t(z) = \left(Re(e^{it}(h(z) + g(z))), Im(e^{it}(h(z) - g(z))), 2Im\left\{ e^{it} \int_0^z q(\xi) h'(\xi) d\xi \right\} \right).$$

In particular, X_0 and $X_{\pi/2}$ are conjugate minimal surfaces and for each $t \in (0,\pi/2)$ is an associated surface of X_0.

In this article, we consider some normalized functions that map $\mathbb{D}$ conformally onto the interior of certain convex regions, such as the right half of a hyperbola, the Lemniscate of Bernoulli, and the parabola. To study the geometrical interpretations of those functions, we first set

$$\phi_1(z) = 2\left(\frac{1}{\sqrt{1-z}} - 1\right), \qquad (z \in \mathbb{D}).$$

ϕ_1 is a doubly valued function. Therefore, we consider the principal branch, where the function is analytic and single valued. Note that on $|z| = 1$, we have

$$w = \phi_1(e^{i\theta}) = 2\left(\frac{1}{\sqrt{1-e^{i\theta}}} - 1\right),\ (0 \le \theta \le 2\pi).$$

This implies that

$$\left|1 - \frac{4}{(w+2)^2}\right| = 1. \tag{1.1}$$

Setting $w = u + iv$ in (1.1), we conclude that ϕ_1 represents the interior of the right half branch of a hyperbolic region given by

$$\Omega_1 := \{u+iv \in \mathbb{C} : (u^2+v^2)((u+4)^2+v^2) - ((u+2)^2+v^2) - 1 = 0\}. \tag{1.2}$$

Similarly, by considering the function $\phi_2(z) = 2(\sqrt{1+z} - 1)$, $z \in \mathbb{D}$, we observe that $\phi_2(\mathbb{D})$ represents interior of the right half of the Lemniscate Bernoulli Ω_2, that is

$$\Omega_2 := \{u+iv \in \mathbb{C} : (u^2+v^2)((u+4)^2+v^2) < 16\}. \tag{1.3}$$

We are also interested in studying certain parabolic regions whose shear can be lifted to a minimal surface. Thus, upon considering

$$\widetilde{\phi_3}(z) = 1 + \frac{2}{\pi^2}\left(\log\left(\frac{1+\sqrt{z}}{1-\sqrt{z}}\right)\right)^2 = 1 + \frac{8}{\pi^2}z + \frac{16}{3\pi^2}z^2 + \frac{184}{45\pi^2}z^3 + \cdots, \quad (z \in \mathbb{D}),$$

it is observed that, $\widetilde{\phi_3}$ is a many valued function. To make it single-valued analytic, the branch of $\sqrt{z}$ is so chosen such that $Im(\sqrt{z}) \ge 0$. Furthermore, $\widetilde{\phi_3}$ is a member of the class with positive real parts and maps $\mathbb{D}$ into the parabolic region $\widetilde{\Omega_3}$, where $\widetilde{\Omega_3} := \{u+iv \in \mathbb{C} : u^2 > (u-1)^2 + v^2\}$. Set

$$\phi_3(z) = \frac{\pi^2}{8}(\widetilde{\phi_3} - 1) = \frac{1}{4}\left(\log\left(\frac{1+\sqrt{z}}{1-\sqrt{z}}\right)\right)^2, \quad (z \in \mathbb{D}).$$

$\phi_3(z)$ is a member of the family $\mathscr{S}$ and maps $\mathbb{D}$ onto the interior of a parabolic region.

The article is structured as follows. In Section 1, the basic geometric structures of the domains are thoroughly studied, and the fundamental results used as a methodology in proving our main results are discussed. Section 2 focuses on the generation of minimal surfaces lying over the shear of a hyperbolic domain. Minimal surfaces over the shear of a Lemniscate Bernoulli and a parabolic domain are well studied in Sections 3 and 4, respectively. Graphical illustrations of the results found in different sections are done in Section 5.

2. Minimal Surfaces Associated with a Hyperbolic Domain

In this section, we find the projection map $f_1 = h_1 + \overline{g_1}$ of the minimal surface lying over shear of the interior of right half branch of the hyperbola defined in (1.2). We also find representations of the corresponding minimal surfaces.

Theorem 2.1. *Let $\phi_1(z) = h_1(z) - g_1(z) = 2\left(\frac{1}{\sqrt{1-z}} - 1\right)$, which maps the unit disk $\mathbb{D}$ onto a right half of hyperbola defined as in (1.2). Then for a given square dilatation $w = z^2$, the minimal surface lying over the shear of $\phi_1(\mathbb{D})$ is*

$$X_1 = (Re(h_1(z) + g_1(z)),\ Im(h_1(z) - g_1(z)),\ 2Im\Psi_1(z)),$$

and the corresponding harmonic projection map $f_1 = h_1 + \overline{g_1}$ belongs to the family $\mathscr{S}^0_{\mathscr{H}}$ with $h_1(0) = g_1(0) = g_1'(0) = h_1'(0) - 1 = 0$,

$$h_1(z) = \frac{5-3z}{3(1-z)^{3/2}} + \frac{1}{2\sqrt{2}}\log\left(\frac{\sqrt{2}-\sqrt{1-z}}{\sqrt{2}+\sqrt{1-z}}\right) - \frac{1}{2\sqrt{2}}\log\left(\frac{\sqrt{2}-1}{\sqrt{2}+1}\right) - \frac{5}{3},$$

$$g_1(z) = \frac{3z-1}{3(1-z)^{3/2}} + \frac{1}{2\sqrt{2}}\log\left(\frac{(\sqrt{2}-\sqrt{1-z})(\sqrt{2}+1)^2}{\sqrt{2}+\sqrt{1-z}}\right) + \frac{1}{3}$$

and

$$\Psi_1(z) = \frac{3z-1}{6(1-z)^{3/2}} - \frac{1}{4\sqrt{2}}\log\left(\frac{\sqrt{2}-\sqrt{1-z}}{\sqrt{2}+\sqrt{1-z}}\right) + c_1,$$

where c_1 is a constant.

Proof. For $z \in \mathbb{D}$, we have

$$Re\left(1 + \frac{z\phi_1''(z)}{\phi_1'(z)}\right) = Re\left(1 + \frac{3}{2}\left(\frac{z}{1-z}\right)\right) > \frac{1}{4}.$$

Thus, ϕ_1 is convex in $\mathbb{D}$. In particular, $\phi_1(\mathbb{D})$ is a CHD. We may note that $\phi_1(z) \in \mathscr{S}$, the class of normalized analytic univalent functions.

Next, we proceed to show that f_1 is a member of the subfamily of harmonic mappings $\mathscr{S}^0_{\mathscr{H}}$. Considering

$$\phi_1(z) = h_1(z) - g_1(z) = 2\left(\frac{1}{\sqrt{1-z}} - 1\right), \qquad (z \in \mathbb{D}) \tag{2.1}$$

and the dilatation $w = g_1'/h_1' = z^2$, we have $h_1'(z) = \frac{1}{(1+z)(1-z)^{5/2}}$. Thus,

$$h_1(z) = \frac{5-3z}{6(1-z)^{3/2}} + \frac{1}{4}\int \frac{dz}{(1+z)(1-z)^{1/2}}.$$

Note that

$$\frac{d}{dz}\left[\frac{\sqrt{2}}{8}\log\left(\frac{\sqrt{2}-\sqrt{1-z}}{\sqrt{2}+\sqrt{1-z}}\right)\right] = \frac{\sqrt{2}}{8}\left[\frac{\frac{1}{2\sqrt{1-z}}}{\sqrt{2}-\sqrt{1-z}} - \frac{\frac{-1}{2\sqrt{1-z}}}{\sqrt{2}+\sqrt{1-z}}\right]$$
$$= \frac{\sqrt{2}}{16\sqrt{1-z}}\left[\frac{(\sqrt{2}+\sqrt{1-z})+(\sqrt{2}-\sqrt{1-z})}{1-z}\right]$$
$$= \frac{1}{4(1+z)\sqrt{1-z}}.$$

Therefore, we have

$$h_1(z) = \frac{5-3z}{6(1-z)^{3/2}} + \frac{1}{4\sqrt{2}}\log\left(\frac{\sqrt{2}-\sqrt{1-z}}{\sqrt{2}+\sqrt{1-z}}\right) + k_1, \tag{2.2}$$

where k_1 is a constant. To meet the required normalization conditions $h_1(0)=0$ and $h_1'(0)=1$, we scale $h_1(z)$ given in (2.2) by 2, and then translate that by $\frac{-5}{6} - \frac{\sqrt{2}}{8}\log\left(\frac{\sqrt{2}-1}{\sqrt{2}+1}\right)$. Thus, we have

$$h_1(z) = \frac{5-3z}{3(1-z)^{3/2}} + \frac{1}{2\sqrt{2}}\log\left(\frac{\sqrt{2}-\sqrt{1-z}}{\sqrt{2}+\sqrt{1-z}}\right) - \frac{1}{2\sqrt{2}}\log\left(\frac{\sqrt{2}-1}{\sqrt{2}+1}\right) - \frac{5}{3}. \tag{2.3}$$

From (2.3) and (2.1), we obtain

$$g_1(z) = \frac{3z-1}{3(1-z)^{3/2}} + \frac{1}{2\sqrt{2}}\log\left(\frac{(\sqrt{2}-\sqrt{1-z})(\sqrt{2}+1)^2}{\sqrt{2}+\sqrt{1-z}}\right) + \frac{1}{3}. \tag{2.4}$$

The harmonic projection mapping $f_1 = h_1 + \overline{g_1}$, where h_1 and g_1 are given as above, admits a square dilatation $w = z^2,\ |w|<1$, and $g_1(0)=0$. Therefore, we have $f_1 \in \mathscr{S}^0_{\mathscr{H}}$. By the use of Weierstrass Representation Theorem 1.1, the minimal graph associated with the harmonic mapping f_1 is given by

$$X_1 = (x_1,x_2,x_3) = (Re(h_1(z)+g_1(z)), Im(h_1(z)-g_1(z)), 2Im(\Psi_1(z))), \tag{2.5}$$

where $h_1(z)$ and $g_1(z)$ are given by (2.3) and (2.4) respectively and $\Psi_1(z)$ is computed as follows.

$$\Psi_1(z) = \int_0^z z h_1'(\eta)\,d\eta = \int_0^z \frac{\eta}{(1+\eta)(1-\eta)^{5/2}}\,d\eta$$
$$= \frac{3z-1}{6(1-z)^{3/2}} - \frac{\sqrt{2}}{8}\log\left(\frac{\sqrt{2}-\sqrt{1-z}}{\sqrt{2}+\sqrt{1-z}}\right) + c_1. \tag{2.6}$$

This completes the proof of Theorem 2.1. □

It is observed from the proof of Theorem 2.1 that ϕ_1, defined by (2.1), is a convex function and also a member of the class $\mathscr{S}$. Thus, by Theorem 1.2, we find the conjugate minimal surface of the minimal surface X_1 and its harmonic projection mapping to its base plane.

Corollary 2.2. *The conjugate minimal surface of X_1 is given by*

$$(X_1)_{conj} = (Im(h_1(z)+g_1(z)),\ Re(h_1(z)-g_(z)),\ 2Re(\Psi_1(z))), \tag{2.7}$$

where $h_1(z)$, $g_1(z)$ and $\Psi_1(z)$ are respectively given in (2.3), (2.4) and (2.6) . The corresponding harmonic projection map of X_1 is $F_1(z) = ih_1(z) + \overline{ig_1(z)}$, $z \in \mathbb{D}$.

Remark 2.3. The following expression gives the associated minimal surfaces of the minimal surfaces X_1 and $(X_1)_{conj}$ are $Z_1 = (\cos t)X_1 + (\sin t)(X_1)_{conj}$, $0 \le t \le \pi/2$, where X_1 and $(X_1)_{conj}$ are given by (2.5) and (2.7) respectively.

3. Minimal Surfaces Associated with a Lemniscate of Bernoulli

This section is devoted to representing the minimal surface lying over the shear of the interior of the right half branch of the Lemniscate of Bernoulli Ω_2 defined in (1.3), in explicit form.

Theorem 3.1. *Let $\phi_2(z) = h_2(z) - g_2(z) = 2(\sqrt{1+z} - 1)$, which maps the unit disk $\mathbb{D}$ onto a right half of the Lemniscate of Bernoulli Ω_2. Then for square dilatation $w = h'/g' = z^2$, the minimal surface lying over the shear of Ω_2 is*

$$X_2 = (Re(h_2(z) + g_2(z)),\ Im(h_2(z) - g_2(z)),\ 2Im\Psi_2(z)),$$

and the corresponding harmonic projection map is $f_2(z) = h_2(z) + \overline{g_2(z)}$, $z \in \mathbb{D}$, with $h_2(0) = g(0) = g_2'(0) = h_2'(0) - 1 = 0$,

$$h_2(z) = \frac{-1}{\sqrt{1+z}} + \frac{1}{2\sqrt{2}} \log\left(\frac{\sqrt{2}+\sqrt{1+z}}{\sqrt{2}-\sqrt{1+z}}\right) - \frac{1}{\sqrt{2}}\log(\sqrt{2}+1) + 1, \tag{3.1}$$

$$g_2(z) = \frac{-(3+2z)}{\sqrt{1+z}} + \frac{1}{2\sqrt{2}} \log\left(\frac{\sqrt{2}+\sqrt{1+z}}{(\sqrt{2}-\sqrt{1+z})(\sqrt{2}+1)^2}\right) + 3, \tag{3.2}$$

and

$$\Psi_2(z) = \frac{1}{\sqrt{1+z}} + \frac{1}{2\sqrt{2}} \log\left(\frac{\sqrt{2}+\sqrt{1+z}}{\sqrt{2}-\sqrt{1+z}}\right) + c_2,$$

where c_2 is a constant.

Proof. Consider

$$h_2(z) - g_2(z) = 2(\sqrt{1+z} - 1), \qquad (z \in \mathbb{D}), \tag{3.3}$$

and

$$w_2(z) = g_2'(z)/h_2'(z) = z^2. \tag{3.4}$$

From (3.3), we have

$$h_2'(z) - g_2'(z) = \frac{1}{\sqrt{1+z}}. \tag{3.5}$$

Solving equations (3.4) and (3.5) for $h_2'(z)$, we have

$$h_2'(z) = \frac{1}{(1-z)(1+z)^{3/2}}. \tag{3.6}$$

Integration of (3.6) yields

$$h_2(z) = \frac{-1}{\sqrt{1+z}} + \frac{1}{2\sqrt{2}} \log\left(\frac{\sqrt{2}+\sqrt{1+z}}{\sqrt{2}-\sqrt{1+z}}\right) + k_2. \tag{3.7}$$

Employing the normalization conditions $h_2(0) = 0$ and $h'(0) = 1$, in (3.7) we compute k_2 as,

$$k_2 = 1 - \frac{1}{\sqrt{2}} \log(\sqrt{2}+1).$$

Thus, we have $h_2(z)$ is as given in (3.1). Similarly, solving the equations (3.4) and (3.5) for $g'(z)$ and then integrating, we obtain $g_2(z)$ as given in (3.2). From the Weierstrass representation theorem, the minimal surface lying over the shear of right half of the Lemniscate of Bernoulli is given by,

$$X_2 = (\widehat{x_1}, \widehat{x_2}, \widehat{x_3}) = (Re(h_2(z) + g_2(z)),\ Im(h_2(z) - g_2(z)),\ 2Im(\Psi_2(z))), \tag{3.8}$$

where $h_2(z)$ and $g_2(z)$ are given by (3.1) and (3.2) respectively and $\Psi_2(z)$ is computed as follows.

$$\begin{aligned}\Psi_2(z) &= \int_0^z z h_2'(\eta) d\eta = \int_0^z \frac{\eta}{(1+\eta)(1-\eta)^{3/2}} d\eta \\ &= \frac{1}{\sqrt{1+z}} + \frac{1}{2\sqrt{2}} \log\left(\frac{\sqrt{2}+\sqrt{1+z}}{\sqrt{2}-\sqrt{1+z}}\right) + c_2. \end{aligned} \tag{3.9}$$

This completes the proof of Theorem 3.1. □

Corollary 3.2. *The conjugate minimal surface of X_2, is given by*

$$(X_2)_{conj} = (Im(h_2(z) + g_2(z)),\ Re(h_2(z) - g_2(z)),\ 2Re(\Psi_2(z))), \tag{3.10}$$

where $h_2(z), g_2(z)$ and $\Psi_2(z)$ are given in (3.1),(3.2) and (3.9) respectively. The corresponding harmonic projection map of X_2 is $F_2(z) = ih_2(z) + \overline{ig_2(z)}$.

Remark 3.3. The expression of associated minimal surfaces of the minimal surfaces X_2 and $(X_2)_{conj}$ are given by $Z_2 = (\cos t)X_2 + (\sin t)(X_2)_{conj}$, $0 \le t \le \pi/2$, where X_2 and $(X_2)_{conj}$ are given by (3.8) and (3.10) respectively.

4. Minimal Surfaces Associated with a Parabolic Domain

Following the same approach as the previous sections, we also find the minimal surface over shear of a parabolic region.

Theorem 4.1. *Let $\phi_3(z) = h_3(z) - g_3(z) = \frac{1}{4}\left(\log\left(\frac{1+\sqrt{z}}{1-\sqrt{z}}\right)\right)^2$, which maps the unit disk $\mathbb{D}$ onto the interior of a parabolic region. Then, for the dilatation $w = z^2$, the minimal surface lying over the shear of $\phi_3(\mathbb{D})$ is*

$$X_3 = (Re(h_3(z) + g_3(z)),\ Im(h_3(z) - g_3(z)),\ 2Im\Psi_3(z)),$$

and the corresponding harmonic projection map is $f_3(z) = h_3(z) + \overline{g_3(z)}$, $z \in \mathbb{D}$, where

$$\begin{aligned} h_3(z) =& \frac{1}{4}\log\left(\frac{1+\sqrt{z}}{1-\sqrt{z}}\right)\left(\frac{z+\sqrt{z}-1}{1-z} + \log\left(\frac{1+\sqrt{z}}{1-\sqrt{z}}\right)\right) - \frac{1}{8}\left(\frac{1+z}{1-z}\right) \\ &+ \frac{i}{8}\Big(\log\left(\frac{2\sqrt{z}-i(1-z)}{1+z}\right) + Li_2\left(1 - \frac{i(1+\sqrt{z})}{1-\sqrt{z}}\right) \\ &- Li_2\left(1 + \frac{i(1+\sqrt{z})}{1-\sqrt{z}}\right)\Big), \end{aligned} \tag{4.1}$$

$$g_3(z) = \frac{1}{4}\left(\frac{z+\sqrt{z}-1}{1-z}\right)\log\left(\frac{1+\sqrt{z}}{1-\sqrt{z}}\right) - \frac{1}{8}\left(\frac{1+z}{1-z}\right) + \frac{i}{8}\Big(\log\left(\frac{2\sqrt{z}-i(1-z)}{1+z}\right) + Li_2\left(1-\frac{i(1+\sqrt{z})}{1-\sqrt{z}}\right) - Li_2\left(1+\frac{i(1+\sqrt{z})}{1-\sqrt{z}}\right)\Big), \tag{4.2}$$

and

$$\Psi_3(z) = \int_0^z \frac{\sqrt{\eta}}{2(1-\eta)^2(1+\eta)}\log\left(\frac{1+\sqrt{\eta}}{1-\sqrt{\eta}}\right)d\eta.$$

Proof. Let $\phi_3(z) = \frac{1}{4}\left(\log\left(\frac{1+\sqrt{z}}{1-\sqrt{z}}\right)\right)^2, \quad (z \in \mathbb{D})$. Then, we have

$$Re\left(1+\frac{\phi_3''(z)}{\phi_3'(z)}\right) = Re\left(1+\frac{2\sqrt{z}+(3z-1)\log\left(\frac{1+\sqrt{z}}{1-\sqrt{z}}\right)}{2z(1-z)\log\left(\frac{1+\sqrt{z}}{1-\sqrt{z}}\right)}\right) > Re\left(1-\frac{2i-4\log\left(\frac{1+i}{1-i}\right)}{4\log\left(\frac{1+i}{1-i}\right)}\right) = 2-\frac{1}{\pi} > 0.$$

Therefore, $\phi_3(z)$ is convex, and hence in particular it is univalent and convex in horizontal direction. Write

$$\phi_3(z) = h_3(z) - g_3(z) = \frac{1}{4}\left(\log\left(\frac{1+\sqrt{z}}{1-\sqrt{z}}\right)\right)^2. \tag{4.3}$$

On differentiation, we have

$$\phi_3'(z) = h_3'(z) - g_3'(z) = \frac{1}{2(1-z)\sqrt{z}}\log\left(\frac{1+\sqrt{z}}{1-\sqrt{z}}\right). \tag{4.4}$$

Further, square dilatation implies that

$$g_3'(z) = z^2 h_3'(z), \quad (z \in \mathbb{D}). \tag{4.5}$$

Solving (4.4) and (4.5) for $g_3'(z)$ and then integrating from 0 to z, we obtain

$$g_3(z) = \int_0^z \frac{\eta\sqrt{\eta}}{2(1+\eta)(1-\eta)^2}\log\left(\frac{1+\sqrt{\eta}}{1-\sqrt{\eta}}\right)d\eta.$$

After simplification of the above integral, we get

$$g_3(z) = \frac{1}{4}\left(\frac{z+\sqrt{z}-1}{1-z}\right)\log\left(\frac{1+\sqrt{z}}{1-\sqrt{z}}\right) - \frac{1}{8}\left(\frac{1+z}{1-z}\right) + \frac{i}{8}\Big(\log\left(\frac{2\sqrt{z}-i(1-z)}{1+z}\right) + Li_2\left(1-\frac{i(1+\sqrt{z})}{1-\sqrt{z}}\right) - Li_2\left(1+\frac{i(1+\sqrt{z})}{1-\sqrt{z}}\right)\Big),$$

where $Li_2(z)$ represents the Spence's function or Dilogarithm of z. Employing the expression of $g_3(z)$ in (4.3), we obtained the expression of $h_3(z)$ as in (4.1). The theorem due to Clunie and Sheil-Small ascertains that the harmonic projection map $f_3(z) := h_3(z) + \overline{g_3(z)}$ is univalent.

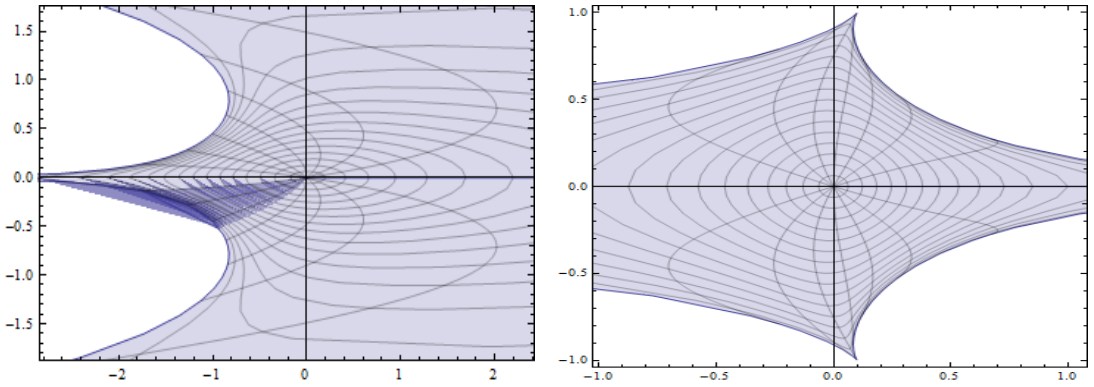
Furthermore, from Theorem 1.1, the minimal surface lying over the shear of interior of the parabolic region is given by,

$$X_3 = (\widetilde{x}_1, \widetilde{x}_2, \widetilde{x}_3) = (Re(h_3(z) - g_3(z),\ Im(h_3(z) + g_3(z))),\ 2Im(\Psi_3(z))),$$

where $h_3(z)$ and $g_3(z)$ are given by (4.1) and (4.2) respectively, and $\Psi_3(z)$ is computed as follows.

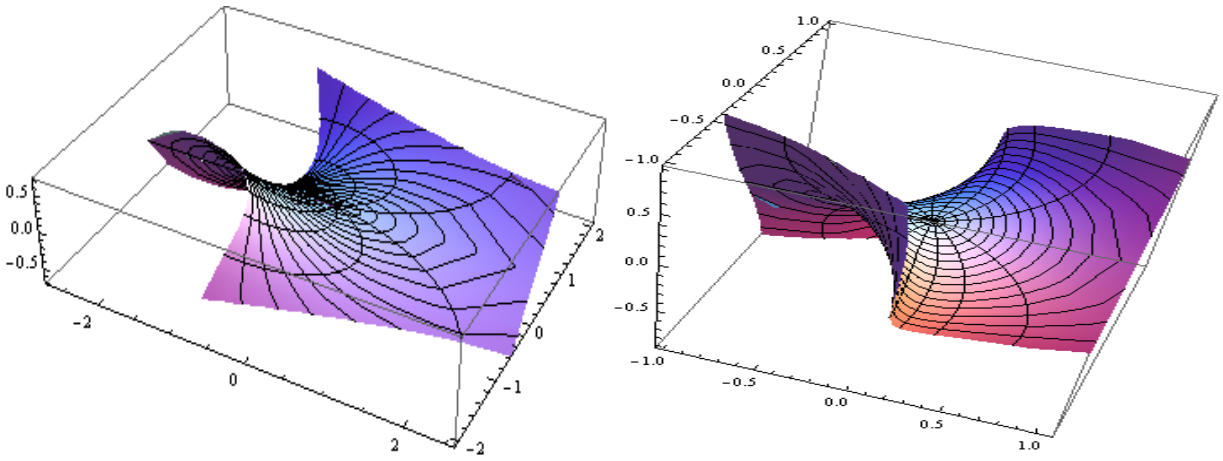
$$\Psi_3(z) = \int_0^z z h_3'(\eta) d\eta = \int_0^z \frac{\sqrt{\eta}}{2(1-\eta)^2(1+\eta)} \log\left(\frac{1+\sqrt{\eta}}{1-\sqrt{\eta}}\right) d\eta.$$

This completes the proof of Theorem 4.1. □



(a) f_1 given in Theorem 2.1 (b) f_2, given in Theorem 3.1

FIGURE 1. Harmonic projection map



(a) X_1 associated with f_1 (b) X_2 associated with f_2

FIGURE 2. Minimal surfaces

5. ILLUSTRATIONS

In this section, we present geometric representations of minimal surfaces and their associated harmonic projection mappings using Mathematica 9. Figure 1(a) illustrates the harmonic projection mapping f_1 as defined in Theorem 2.1, with the corresponding minimal surface X_1 depicted in Figure 2(a). Similarly, Figure 1(b) shows the harmonic projection mapping f_2 established in Theorem 3.1, while the associated minimal surface X_2 is presented in Figure 2(b). The construction of additional minimal surfaces follows analogous procedures.

6. Conclusion and Future Directions

In this paper, we developed a constructive framework for generating minimal surfaces via harmonic shear of conformal mappings defined on convex domains. Using the Weierstrass–Enneper representation together with the shear construction, we obtained explicit harmonic mappings whose lifts yield new classes of minimal surfaces. In particular, concrete representations were derived for surfaces associated with domains bounded by a hyperbola, the Lemniscate of Bernoulli, and a parabola.

The results highlight the essential role of convexity in ensuring the univalence of the harmonic mappings and the regularity of the corresponding minimal surfaces. The use of square dilatation ensures compatibility with the Weierstrass representation, yielding parametrizations with well-defined geometric behavior. Furthermore, explicit constructions of conjugate and associated minimal surfaces provide a richer geometric structure, yielding continuous families that are connected by harmonic conjugacy. These surfaces may also find applications in areas involving optimal geometric configurations, including physical and natural models.

Future work includes extensions to non-convex and multiply connected domains, where global univalence and area-minimizing properties are more subtle. Further investigation of curvature estimates, stability, completeness, and boundary behavior of the associated minimal surfaces is of interest. The study of more general dilatations and classification of the resulting surfaces also remains open. In addition, the development of computational methods for visualization and approximation may lead to applications in geometric modeling, mathematical physics, and material science.

Acknowledgements

The authors gratefully acknowledge Prof. Priyabrat Gochhayat and Prof. Michel Dorff for their valuable suggestions and careful proofreading during the preparation of this paper. The authors also thank the anonymous reviewers for their insightful comments and constructive suggestions, which have significantly improved the clarity and readability of this paper.

References

[1] J. V. Barth, G. Costantini, K. Kern, Engineering atomic and molecular nanostructures at surfaces, Nature 437 (2005) 671–679.

[2] B. Bhowmik, S. Majee, Curvature estimates for minimal surfaces associated with harmonic mappings having nonzero pole, Complex Variables and Elliptic Equations 71 (2026) 1261-1275.

[3] J. Clunie, T. Sheil-Small, Harmonic univalent functions, Ann. Acad. Sci. Fenn. Ser. A I Math. 9 (1984) 3–25.

[4] M. Dorff, D. Halverson, G. Lawlor, Area-minimizing minimal graphs over nonconvex domains, Pacific J. Math. 210 (2003) 229–259.

[5] M. Dorff, S. Muir, A family of minimal surfaces and univalent planar harmonic mappings, Abstr. Appl. Anal. 2014 (2014) 476061.

[6] M.J. Dorff, Harmonic univalent mappings onto asymmetric vertical strips, In: Computational Methods and Function Theory 1997, vol. 11 of Ser. Approx. Decompos. pp. 171–175, World Sci. Publ., River Edge, NJ, 1999.

[7] P. Duren, Harmonic mappings in the plane, vol. 156 of Cambridge Tracts in Mathematics, Cambridge University Press, Cambridge, 2004.

[8] K. Jaglan, A. Sairam Kaliraj, Area-minimizing minimal graphs over linearly accessible domains, J. Geom. Anal. 33 (2023) 321.

[9] S.H. Jun, Mappings related to minimal surfaces, J. Chungcheong Math. Soc. 194 (2006) 313–313.

[10] D. Kalaj, Harmonic univalent functions and minimal surfaces, Complex Var. Elliptic Equ. 66 (2021) 777–795.
[11] H. Lewy, On the non-vanishing of the Jacobian in certain one-to-one mappings, Bull. Amer. Math. Soc. 42 (1936) 689–692.
[12] L. Li, S. Ponnusamy, M. Vuorinen, The minimal surfaces over the slanted half-planes, vertical strips and single slit, In: Current Topics in Pure and Computational Complex Analysis, Trends Math. pp. 47–61, Birkhäuser/Springer, New Delhi, 2014.
[13] P. Morgan, Geometric Measure Theory, fifth ed. Elsevier/Academic Press, Amsterdam, 2016.
[14] R. Osserman, A Survey of Minimal Surfaces, second ed. Dover Publications, Inc., New York, 1986.
[15] S. Ponnusamy, T. Quach, A. Rasila, Harmonic shears of slit and polygonal mappings, Appl. Math. Comput. 233 (2014) 588–598.